

Simultaneous Observation of Positive and Negative NOE in Biomolecules: A Bistable Jump Model for Segmental Motion with Modulation of Internuclear Distances[†]

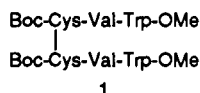
V. V. Krishnan,[‡] S. C. Shekar,[§] and Anil Kumar^{*.†,||}

Contribution from the Department of Physics and Sophisticated Instruments Facility, Indian Institute of Science, Bangalore 500 012, India, and Department of Biophysics and Molecular Biology, Mayo Foundation, Rochester, Minnesota 55905. Received January 15, 1991

Abstract: Recently a negative nuclear Overhauser effect (NOE) among the backbone protons as well as a positive NOE between the backbone and ring protons of tryptophan in a peptide was reported. While the negative NOE is indicative of slow overall reorientation of the molecule, simultaneous occurrence of a positive NOE is indicative of internal motions in the molecule. To explain these observations we develop here a model in which the overall motion is anisotropic reorientation and the internal motion modulates the internuclear distance. Analytical expressions for the spectral density functions for dipole-dipole relaxation are obtained when the internal motion is a bistable jump. Steady-state and transient NOE calculations are performed for two relaxation-coupled spins. The results confirm that when the overall motion is in the slow motion limit and the side chain internal motion is in the fast motion limit, the NOE within the backbone protons is negative and that between the backbone and the side chain protons is positive. This model further shows that the NOE between the backbone and the side chain is proportional to the weighted average of the inverse sixth power of the distance between the interacting spins only when the overall motion is isotropic, dominates the relaxation process and is much faster than the internal motion. With use of this model, multispin steady-state NOE's are computed to explain the experimental observation of positive and negative NOE's and their temperature dependence in a tryptophan-containing polypeptide.

I. Introduction

¹H-¹H nuclear Overhauser effect (NOE) spectroscopy is an important tool for the study of structure and dynamics in organic molecules and biomolecules.¹⁻⁴ This unique method, which can determine the three-dimensional structure of molecules in solution, has in recent years become of central importance among NMR spectroscopists.⁴⁻⁶ The magnitude and the sign of NOE's are crucially dependent on the motional rates represented by the correlation time of reorientation (τ_c) and the Larmor frequency (ω). Under the assumption of isotropic random reorientation of the molecule the NOE between two mutually relaxing spins is positive for fast reorientations ($\omega\tau_c \ll 1$, also known as the short correlation limit) and negative for slow reorientations ($\omega\tau_c \gg 1$, the long correlation or spin diffusion limit).⁷ Recently in a polypeptide



negative NOE was reported among the backbone protons and positive NOE between the backbone and the ring protons.⁸ This situation is indicative of internal motions, and the estimation of the NOE between the backbone and the ring protons is not straightforward. To explain these observations in detail, in the present paper we build a model which includes anisotropic reorientation of the whole molecule with segmental motion of a portion with modulation of internuclear distances. While the spectral densities have been calculated analytically for a general internal motion, the results are discussed in detail for a bistable jump, since, in the present case, the motion of the ring protons is of interest.

A large number of models have been proposed to account for internal motions in relaxation studies. Woessner laid the ground work in this field by first giving a model having isotropic reorientation with internal motion and later generalized it to anisotropic reorientation.⁹⁻¹¹ Internal motion has been treated as continuous diffusion,¹²⁻¹⁴ restricted diffusion,¹⁵⁻¹⁷ lattice jumps,^{12,16-18} wobbling

in a cone,¹⁹ and libration in a cone.²⁰ Applications of these models have also been widely reviewed.²¹ Other "model free" approaches that include internal motion as effective order parameters have also been proposed.²²⁻²⁴ Modulation of the distance between the

- (1) Noggle, J. H.; Schirmer, R. E. *The Nuclear Overhauser Effect: Chemical applications*; Academic Press: New York, 1971.
- (2) Wüthrich, K. *NMR in Biological Research, peptides and proteins*; North Holland: Amsterdam, 1976.
- (3) Wüthrich, W. *NMR of proteins and nucleic acids*; John Wiley and Sons: New York, 1986.
- (4) Anil Kumar *Proc. Indian Acad. Sci. (Chem. Sci.)* **1985**, *95*, 1-8.
- (5) Gao, X.; Patel, D. J. *Q. Rev. Biophys.* **1989**, *22*, 93-138.
- (6) Clore, G. M.; Gronenborn, A. M. *Crit. Rev. Biophys. Mol. Biol.* **1989**, *24*, 479-564.
- (7) Ernst, R. R.; Bodenhausen, G.; Wokaun *Principles of Nuclear Magnetic Resonance in One and Two Dimensions*; Oxford University Press: London, 1986; pp 516.
- (8) Uma, K.; Balaran, H.; Raghobama, S.; Balaran, P. *Biochem. Biophys. Res. Commun.* **1988**, *151*, 153-157.
- (9) Woessner, D. E. *J. Chem. Phys.* **1962**, *36*, 1-4.
- (10) Woessner, D. E. *J. Chem. Phys.* **1968**, *37*, 647-654.
- (11) Woessner, D. E.; Snowden, B. S.; Meyer, G. H. *J. Chem. Phys.* **1969**, *50*, 719-721.
- (12) Wallach, D. *J. Chem. Phys.* **1967**, *47*, 5258-5268.
- (13) Levine, Y. K.; Partington, P.; Roberts, G. C. K. *Mol. Phys.* **1973**, *25*, 497-514.
- (14) Levine, Y. K.; Birdsall, N.; Lee, A. G.; Metcalfe, J. C.; Partington, P.; Roberts, G. C. K. *J. Chem. Phys.* **1974**, *60*, 2890-2899.
- (15) London, R. E.; Avitabile, J. *J. Am. Chem. Soc.* **1978**, *100*, 7159-7165.
- (16) Witterbort, R. J.; Szabo, A. *J. Chem. Phys.* **1978**, *69*, 1722-1736.
- (17) Witterbort, R. J.; Szabo, A.; Gurd, F. R. N. *J. Am. Chem. Soc.* **1980**, *102*, 5723-5728.
- (18) London, R. E.; Avitabile, J. *J. Am. Chem. Soc.* **1977**, *99*, 7765-7776.
- (19) Richarz, R.; Nagayama, K.; Wüthrich, K. *Biochemistry* **1980**, *19*, 5189-5196.
- (20) (a) Howarth, O. W. *J. Chem. Soc., Faraday Trans.* **1978**, *74*, 1031-1041. (b) Howarth, O. W. *J. Chem. Soc., Faraday Trans.* **1979**, *75*, 863-873.
- (21) (a) Healy, F. *Prog. NMR Spectrosc.* **1979**, *13*, 47-85. (b) Lambert, J. B.; Nienhuis, R. J.; Keepers, J. W. *Angew. Chem., Int. Ed. Engl.* **1981**, *20*, 487-500. (c) London, R. E. *Magnetic Resonance in Biology*; Cohen, J. S., Ed.; John Wiley and Sons: New York, 1980; Vol. 1, p 1. (d) Hertz, H. G. *Prog. NMR Spectrosc.* **1983**, *16*, 115-162. (e) Healy, F. *Annu. Rep. NMR Spectrosc.* **1986**, *17*, 179-230.
- (22) (a) Lipari, G.; Szabo, A. *J. Am. Chem. Soc.* **1982**, *104*, 4546-4559. (b) Lipari, G.; Szabo, A. *J. Am. Chem. Soc.* **1982**, *104*, 4559-4570.
- (23) Jardetzky, O. *NMR and Biochemistry*; Opella, S. J., Lu, P., Eds.; Marcel Dekker: New York, 1979; p 141.

[†] Presented in part at the XIV International Conference on Magnetic Resonance in Biological Systems, Warwick, U.K., September 1990.

[‡] Department of Physics, Indian Institute of Science.

[§] Mayo Foundation.

^{||} Sophisticated Instruments Faculty, Indian Institute of Science.

interacting spins due to internal motion was treated in the following studies. Woessner treated the case of two methyl groups internally reorienting independently.²⁵ Tsutsumi²⁶ and Bluhm²⁷ calculated the case of internal motion between three nonequivalent sites, while John et al. treated it as a stochastic diffusion.²⁸ Tropp²⁹ has also investigated the effect of fluctuating internuclear distances, and these results have been used in ³¹P-¹H relaxation studies in DNA.³⁰

Bistable jump motional models are of particular interest in view of the proline and other ring conformations.^{15,18,31-35} The bistable jump model proposed by London et al.^{15,18,31} and later modified by Shekar et al.^{32,33} is utilized to explain the ¹³C relaxation time measurement in the proline molecule. Sarkar et al.³⁴ have also studied the conformational flexibilities of deuterated proline in solid-state NMR spectroscopy, while recently Mádi et al.³⁵ have explicitly used modern NMR methodology in combination with the ¹³C relaxation time measurements to study the conformation of the four proline residues in antamanide.

In this paper analytical expressions for the correlation function are obtained for the general case when the overall motion is anisotropic rotational diffusion and the segmental motion modulates the internuclear distance and is independent of the overall motion. These calculations are aimed at understanding the nuclear Overhauser effect and utilize bistable jump as a model for the internal motion. The spectral density functions are calculated on the basis of the method of Woessner. These calculations clearly show that the transfer of NOE in the presence of segmental motion is governed by the weighted average of the inverse sixth power of the distances between the spins only when the overall motion is isotropic and is fast compared to the internal motion. Both steady-state and transient NOE's have been calculated by using the model for the two-spin system. The simultaneous observation of positive and negative steady-state NOE's in the tryptophan-containing polypeptide and its temperature dependence are explained. Section II contains the calculations of the general spectral density functions, and section III contains the analytical expressions for the spectral density functions when the overall motion is anisotropic rotational diffusion and the internal motion is a bistable jump. In section IV the effects of dynamic parameters involved in the two-spin steady state and transient NOE experiments are presented, while section V discusses experimental results.

II. Theory

The correlation function for anisotropic rotational diffusion of the overall motion of the molecule, with internal motion independent of the overall motion, is obtained by using the method described by Woessner.^{10,11} The nature of the internal motion is kept general in this section, so that any particular model of internal motion can be assumed as a specific case. Consider the molecular fragment shown in Figure 1 consisting of atoms A, B, C, and D with the vector CD (denoted as \vec{r}_1), making a segmental motion about the BC bond (Z_1 axis). The motion of \vec{r}_1 about BC modulates both direction and magnitude of the internuclear vector AD (denoted as \vec{r}).

The spectral density function of the magnetic dipole-dipole relaxation process is given by the Fourier components of the correlation function $G(\tau)$ as³⁶

$$J_h(\omega) = \int_{-\infty}^{\infty} G_h(\tau) e^{-i\omega\tau} d\tau \quad (1)$$

(24) (a) McCain, D. C.; Markley, J. L. *J. Am. Chem. Soc.* **1986**, *108*, 4259-4264. (b) Dellwo, M. J.; Wand, A. J. *J. Am. Chem. Soc.* **1989**, *111*, 4571-4578. (c) Clore, G. M.; Szabo, A.; Bax, A.; Kay, L. E.; Driscoll, P. C.; Gronenborn, A. M. *J. Am. Chem. Soc.* **1990**, *112*, 4989-4991.

(25) Woessner, D. E. *J. Chem. Phys.* **1965**, *42*, 1855-1859.

(26) Tsutsumi, A. *Mol. Phys.* **1979**, *37*, 111-127.

(27) Bluhm, T. *Mol. Phys.* **1982**, *47*, 475-486.

(28) John, B. K.; McClung, R. E. D. *J. Magn. Reson.* **1982**, *50*, 267-273.

(29) Tropp, J. *J. Chem. Phys.* **1980**, *72*, 6035-6043.

(30) Keepers, J. W.; James, T. L. *J. Am. Chem. Soc.* **1982**, *104*, 929-939.

(31) London, R. E. *J. Am. Chem. Soc.* **1978**, *100*, 2678-2685.

(32) Shekar, S. C.; Easwaran, K. R. K. *Biopolymers* **1982**, *21*, 1479-1487.

(33) Shekar, S. C. Ph.D. Thesis, Indian Institute of Science, 1983.

(34) Sarkar, S. K.; Young, P. K.; Torchia, D. A. *J. Am. Chem. Soc.* **1986**, *108*, 6459-6464.

(35) Mádi, Z. L.; Griesinger, C.; Ernst, R. R. *J. Am. Chem. Soc.* **1990**, *112*, 2909-2914.

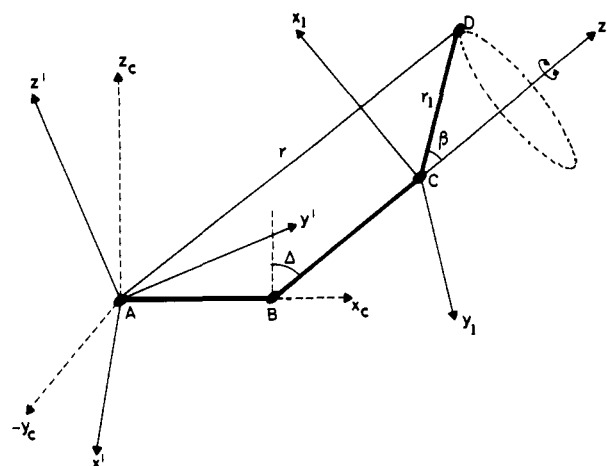


Figure 1. Model molecular fragment considered to calculate the spectral density functions with modulation of internuclear distances due to segmental motion. Atoms A, B, C, and D form the four bonded nuclei in which B and C are the carbons and A and D are the protons between which the NOE is studied. The segmental motion through the B-C bond makes the internuclear vector \overline{AD} time dependent. $S'(X', Y', Z')$ is the molecular fixed frame that undergoes an overall anisotropic rotational reorientation in the laboratory reference frame and a superimposed internal motion, independent of the overall motion about an axis Z_1 in the internal reference frame $S_1(X_1, Y_1, Z_1)$. The angle between the Z axes of these two frames is given by the molecular geometry as $\Delta = \angle ABC - \pi/2$. The vector \vec{r}_1 (which is constant in S_1) makes a polar angle β and an azimuthal angle α in the S_1 frame. The frame $S_C(X_C, Y_C, Z_C)$ is a frame of convenience to calculate the direction cosines of the internuclear vector as described in the Appendix and in Figure 6.

$G(\tau)$, the autocorrelation function of the stationary random process, is defined as³⁶

$$G_h(\tau) = \langle F_h(t) F_h^*(t + \tau) \rangle \quad (2)$$

where $F_h(t)$ are given by

$$\begin{aligned} F_0(t) &= (1 - 3n^2)r^{-3} & F_1(t) &= (l + im)nr^{-3} \\ F_2(t) &= (l + im)^2r^{-3} \end{aligned} \quad (3)$$

l , m , and n are the direction cosines of the internuclear vector in the laboratory coordinate system $S(X, Y, Z)$ and r is the magnitude of the internuclear vector. Thermal motions of the physical system cause $F_h(t)$ to be time dependent via the temporal fluctuations of l , m , n , and r . The angular brackets, $\langle \rangle$, in eq 2 stand for averaging over the random motions.

Denote by $S_0(X_0, Y_0, Z_0)$ a stationary reference frame which is randomly oriented in S , with respect to which the rotational Brownian motion of the molecule is described, and by $S'(X', Y', Z')$ a coordinate frame fixed to the molecule, such that the axes of S' coincide with the three ellipsoidal axes. Let l' , m' , and n' be the direction cosines of the internuclear vector in S' at time t and due to internal motions let l'' , m'' and n'' be the respective direction cosines at a later time $t + \tau$. Also, r' and r'' are the internuclear distances at time t and $t + \tau$, respectively. Following Woessner's treatment,¹⁰ which takes into account the transformation from the molecule fixed frame to S_0 and an isotropic average over all possible orientation of S_0 with respect to S , the autocorrelation function $G(\tau)$ of eq 2 is given by

$$G_h(\tau) = \frac{1}{2} K_h (C_+ \exp(-|\tau|/\tau_+) + C_- \exp(-|\tau|/\tau_-) + C_1 \exp(-|\tau|/\tau_1) + C_2 \exp(-|\tau|/\tau_2) + C_3 \exp(-|\tau|/\tau_3))_{av} \quad (4)$$

in which

$$1/\tau_1 = 4\mathcal{R}_1 + \mathcal{R}_2 + \mathcal{R}_3, \quad 1/\tau_2 = 4\mathcal{R}_2 + \mathcal{R}_1 + \mathcal{R}_3, \quad 1/\tau_3 = 4\mathcal{R}_3 + \mathcal{R}_1 + \mathcal{R}_2 \quad (5)$$

$$C_{\pm} = d \mp e$$

$$\begin{aligned} C_1 &= 6m'n'm''n''r'^{-3}r''^{-3}, & C_2 &= 6l'n'l''n''r'^{-3}r''^{-3}, \\ C_3 &= 6l'm'l''m''r'^{-3}r''^{-3} \end{aligned} \quad (6)$$

with

(36) Abragam, A. *Principles of Nuclear Magnetism*; Oxford University Press: New York, 1961; pp 270-280.

$$d = \frac{1}{2}[3(l'^2l''^2 + m'^2m''^2 + n'^2n''^2) - 1]r'^{-3}r''^{-3}$$

$$e = \frac{1}{2}[\delta_1(l'^2l''^2 + m'^2n''^2 + n'^2m''^2) + \delta_2(m'^2m''^2 + l'^2n''^2 + n'^2l''^2) + \delta_3(n'^2n''^2 + l'^2m''^2 + m'^2l''^2)]r'^{-3}r''^{-3} \quad (7)$$

\mathcal{R}_1 , \mathcal{R}_2 , and \mathcal{R}_3 are the rotational diffusion constants of the ellipsoid about the X' , and Y' , and Z' axes of the S' frame. The values of τ_+ and τ_- are given by

$$1/\tau_{\pm} = 6[\mathcal{R} \pm (\mathcal{R}^2 - \mathcal{L}^2)^{1/2}] \quad (8)$$

where

$$\mathcal{R} = (\mathcal{R}_1 + \mathcal{R}_2 + \mathcal{R}_3)/3 \quad \mathcal{L}^2 = (\mathcal{R}_1\mathcal{R}_2 + \mathcal{R}_1\mathcal{R}_3 + \mathcal{R}_2\mathcal{R}_3)/3 \quad (9)$$

and δ_i in eq 7 are given by

$$\delta_i = (\mathcal{R}_i - \mathcal{R})/\sqrt{\mathcal{R}^2 - \mathcal{L}^2} \quad (10)$$

The constants K_h in eq 4 are defined as

$$K_0 = 1/5; K_1 = 2/15; K_2 = 9/15 \quad (11)$$

The angular bracket $(\langle \rangle)_{av}$ in eq 4 is the average over the values specified by the internuclear vector and the direction cosines due to the internal motion, and the average over the ellipsoidal motion has been taken care of in terms of the constants C_+ , C_- , etc. It is worth mentioning at this point that the cross term between different h values for a single dipolar vector vanishes and has explicitly been proved earlier.³³ The l , m , and n are to be calculated for the given motional model, and by substituting them into eqs 4–10, the correlation function can be obtained.

To characterize the internal rotation, assume a coordinate system $S_1(X_1, Y_1, Z_1)$, where Z_1 is along the internal rotation axis, the B–C, bond as shown in Figure 1. Since the length of r_1 is constant, the time dependence r_1 , introduced about the Z_1 axis due to segmental motion, can be obtained in terms of the time dependence of the azimuthal angle α (see Figure 6 in the Appendix). If $\alpha(t)$ and $\alpha(t + \tau)$ are the azimuthal angles at times t and $t + \tau$ of \bar{r}_1 , respectively, in S_1 , then from the geometry (details are given in the Appendix), the direction cosines of \bar{r} in the reference frame of convenience, S_C , at any instant of time are

$$l_C(t) = (x_0 + k_x \cos \alpha(t))/r(t) \quad m_C(t) = (k_y \sin \alpha(t))/r(t) \quad (12)$$

$$n_C(t) = (z_0 + k_z \cos \alpha(t))/r(t)$$

$r(t)$ is the time-dependent internuclear distance given by

$$r^2(t) = r_0^2 + k_r^2 \cos^2 \alpha(t) \quad (13)$$

The constants defined in eqs 12 and 13 are given by

$$x_0 = r_{AB} + r_{BC} \sin \Delta + r_1 \cos \beta \sin \Delta$$

$$z_0 = r_{BC} \cos \Delta + r_1 \cos \beta \cos \Delta \quad r_0^2 = x_0^2 + z_0^2 + r_1^2 \sin^2 \beta \quad (14)$$

$$k_x = -r_1 \sin \beta \cos \Delta \quad k_y = -r_1 \sin \beta \quad k_z = r_1 \sin \beta \sin \Delta$$

$$k_r^2 = -2r_{AB}r_1 \sin \beta \cos \Delta$$

where r_{AB} and r_{BC} are the interspin distances between the atoms A and B and B and C, respectively, and are time independent, β is the semiangle of the cone of internal motion formed by the Z_1 axis and the vector r_1 , and Δ is given in terms of the molecular geometry as $\angle ABC - \pi/2$ (details in the Appendix). The direction cosines of the internuclear vector in the ellipsoidal frame $S'(X', Y', Z')$ are given by the transformation in the Euler angles (ϕ, ϑ, ψ) from the intermediate reference frame $(S_C(X_C, Y_C, Z_C))$ as

$$\begin{bmatrix} l'(t) \\ m'(t) \\ n'(t) \end{bmatrix} = \begin{bmatrix} a_{11} & a_{12} & a_{13} \\ a_{21} & a_{22} & a_{23} \\ a_{31} & a_{32} & a_{33} \end{bmatrix} \begin{bmatrix} l_C(t) \\ m_C(t) \\ n_C(t) \end{bmatrix} \quad (15)$$

where

$$a_{11} = \cos \psi \cos \phi - \cos \vartheta \sin \phi \sin \psi$$

$$a_{12} = -\sin \psi \cos \phi - \cos \vartheta \sin \phi \cos \psi$$

$$a_{13} = \sin \vartheta \sin \phi$$

$$a_{21} = -\cos \psi \sin \phi + \cos \vartheta \cos \phi \sin \psi$$

$$a_{22} = -\sin \psi \sin \phi + \cos \vartheta \cos \phi \cos \psi$$

$$a_{23} = -\sin \vartheta \cos \phi$$

$$a_{31} = \sin \vartheta \sin \psi$$

$$a_{32} = \sin \vartheta \cos \psi$$

$$a_{33} = \cos \vartheta \quad (16)$$

Similarly $l''(t + \tau)$, $m''(t + \tau)$, and $n''(t + \tau)$ can be defined with the same transformation matrix as given in eq 15. The values ϕ , ϑ , and ψ are specific to the geometry of the molecule and motional model. By substituting for the l , m , and n in eqs 6 and 7 at times t and $t + \tau$ the expression for the correlation time, eq 2 can be written as

$$G(\tau) = \frac{1}{2}K_h \langle Q[l'(t), m'(t), n'(t)|l''(t + \tau), m''(t + \tau), n''(t + \tau)] \rangle_{av} \quad (17)$$

Q can be calculated for a specific model of internal motion, which for a bistable jump is obtained analytically in the next section. The expression of $G(\tau)$ in eq 17 is general and can be extended to more than four atoms in a given framework by successive transformations in Euler angles by considering four atoms to start with, as is done in the case of multiple internal rotations in aliphatic chains.^{13–16}

III. Bistable Jump Model for Internal Motion

Random jump between various stable conformations is an important motional process of relaxation in organic molecules and biomolecules. It is known from the studies of proteins in the solid state that the aromatic moieties undergo a flip motion in the protein matrix, and these motions play an important role in understanding various biological activities.³⁷ The flip motion in the solid state is normally a 180° flip about the C^β – C^γ axis of the amino acids having aromatic side chains and is relatively fast in the residues tyrosine and phenylalanine compared to that in tryptophan.³⁷ Explicit study of the motional aspects of the aromatic residues in basic pancreatic trypsin inhibitor (BPTI) by Wüthrich and co-workers^{38,39} confirms such flip motions even in the liquid state. Hence assuming the internal motion as a flip motion about the C^β – C^γ axis of the aromatic side chain seems appropriate. For an n site jump the Q given in eq 17 can be written as

$$\langle Q \rangle = \sum_{i,j=1}^n Q[l_i(t), m_i(t), n_i(t) | l_j(t + \tau), m_j(t + \tau), n_j(t + \tau)] p(i, t | j, t + \tau) \quad (18)$$

The average in eq 17, due to the internal motion, is determined by weighted summation over all n sites. $p(i, t | j, t + \tau)$ is the probability of finding the system (d - d vector), taking the state i at time t and j at time $t + \tau$,³⁶ and can be written as

$$p(i, t | j, t + \tau) = P(i, t | j, t + \tau) p(i, t) \quad (19)$$

where $P(i, t | j, t + \tau)$ is the conditional probability of the system that takes the state j at time $t + \tau$ when it is known that it takes the state i at time t . For a bistable jump, where the dipolar vector changes its orientation between two possible sites a and b, eq 18 becomes

$$\langle Q \rangle = Q(l_a, m_a, n_a | l_a, m_a, n_a) p(a, t | a, t + \tau) + Q(l_a, m_a, n_a | l_b, m_b, n_b) p(a, t | b, t + \tau) + Q(l_b, m_b, n_b | l_a, m_a, n_a) p(b, t | a, t + \tau) + Q(l_b, m_b, n_b | l_b, m_b, n_b) p(b, t | b, t + \tau) \quad (20)$$

where l_a , m_a , and n_a are the direction cosines of the site a and l_b , m_b , and n_b are those of the site b. Probabilities $p(i, t | j, t + \tau)$ are the probability functions defined in eq 19 and take the following form for a bistable jump model^{31–33}

$$p(a, t | a, t + \tau) = \frac{\tau_a}{(\tau_a + \tau_b)^2} [\tau_a + \tau_b \exp(-|\tau|/\tau_c)]$$

$$p(b, t | b, t + \tau) = \frac{\tau_b}{(\tau_a + \tau_b)^2} [\tau_b + \tau_a \exp(-|\tau|/\tau_c)]$$

$$p(a, t | b, t + \tau) = \frac{\tau_a \tau_b}{(\tau_a + \tau_b)^2} [1 - \exp(-|\tau|/\tau_c)] = p(b, t | a, t + \tau) \quad (21)$$

(37) (a) Gurd, F. R. N.; Rothgeb, T. M. *Adv. Protein Chem.* **1979**, *33*, 73–165. (b) Rice, D. M.; Wittebort, R. J.; Griffin, R. G.; Meirovitch, F.; Stimson, E. R.; Meinwald, Y. C.; Freed, J. H.; Scheraga, H. A. *J. Am. Chem. Soc.* **1981**, *103*, 7707–7710. (c) Gall, C. M.; Cross, T. A.; DiVerdi, J. A.; Opella, S. J. *Proc. Natl. Acad. Sci. U.S.A.* **1982**, *79*, 101–105.

(38) Reference 3, p 7.

(39) Wüthrich, K. *Biological Magnetic Resonance*; Berliner, L. J., Reuben, J., Eds.; Plenum Press: New York, 1981; Vol. 1, p 1.

where τ_a and τ_b are the lifetimes of the dipolar vector in sites a and b, respectively. τ_c is defined as

$$1/\tau_c = 1/\tau_a + 1/\tau_b \quad (22)$$

Utilizing the fact, from eq 21, that $p(a,t|b,t + \tau)$ and $p(b,t|a,t + \tau)$ are equal, eq 20 can be written as

$$\langle Q \rangle = 2Q(l_a, m_a, n_a | l_b, m_b, n_b) p(a, t | b, t + \tau) + Q(l_a, m_a, n_a | l_a, m_a, n_a) p(a, t | a, t + \tau) + Q(l_b, m_b, n_b | l_b, m_b, n_b) p(b, t | b, t + \tau) \quad (23)$$

The first term in eq 23 can be rewritten by using eq 4 as

$$2Q(l_a, m_a, n_a | l_b, m_b, n_b) = \{C_+(l_a, m_a, n_a | l_b, m_b, n_b) \exp(-|\tau|/\tau_+) + C_-(l_a, m_a, n_a | l_b, m_b, n_b) \exp(-|\tau|/\tau_-) + C_1(l_a, m_a, n_a | l_b, m_b, n_b) \exp(-|\tau|/\tau_1) + C_2(l_a, m_a, n_a | l_b, m_b, n_b) \exp(-|\tau|/\tau_2) + C_3(l_a, m_a, n_a | l_b, m_b, n_b) \exp(-|\tau|/\tau_3)\} p(a, t | b, t + \tau) \quad (24)$$

By substituting C 's from eqs 6 and 7, the above equation becomes

$$2Q(l_a, m_a, n_a | l_b, m_b, n_b) = \frac{1}{r_a^3 r_b^3} \{(\Pi^{ab} - \Theta^{ab}) \exp(-|\tau|/\tau_+) + (\Pi^{ab} + \Theta^{ab}) \exp(-|\tau|/\tau_-) + \Gamma_{yz}^{ab} \exp(-|\tau|/\tau_1) + \Gamma_{xz}^{ab} \exp(-|\tau|/\tau_2) + \Gamma_{xy}^{ab} \exp(-|\tau|/\tau_3)\} p(a, t | b, t + \tau) \quad (25)$$

where

$$\begin{aligned} \Pi^{ab} &= [3(x_a^2 x_b^2 + y_a^2 y_b^2 + z_a^2 z_b^2) r_a^{-2} r_b^{-2}] - 1 \\ \Theta^{ab} &= [\delta_1(x_a^2 x_b^2 + y_a^2 y_b^2 + z_a^2 z_b^2) + \delta_2(y_a^2 y_b^2 + x_a^2 z_b^2 + z_a^2 x_b^2) + \delta_3(z_a^2 z_b^2 + x_a^2 y_b^2 + y_a^2 x_b^2)] r_a^{-2} r_b^{-2} \\ \Gamma_{yz}^{ab} &= 12(y_a y_b z_a z_b) r_a^{-2} r_b^{-2} \quad \Gamma_{xz}^{ab} = 12(x_a x_b z_a z_b) r_a^{-2} r_b^{-2} \\ \Gamma_{xy}^{ab} &= 12(x_a x_b y_a y_b) r_a^{-2} r_b^{-2} \end{aligned} \quad (26)$$

where $r_a, r_b, x_a, y_a, z_a, \dots$ are defined in terms of the direction cosines of eqs 12-16. On substituting the probability function from eq 21 in eq 25 one obtains

$$2Q(l_a, m_a, n_a | l_b, m_b, n_b) = \frac{\tau_a \tau_b}{(\tau_a + \tau_b)^2 r_a^3 r_b^3} \{(\Pi^{ab} - \Theta^{ab}) \exp(-|\tau|/\tau_+) + (\Pi^{ab} + \Theta^{ab}) \exp(-|\tau|/\tau_-) + \Gamma_{yz}^{ab} \exp(-|\tau|/\tau_1) + \Gamma_{xz}^{ab} \exp(-|\tau|/\tau_2) + \Gamma_{xy}^{ab} \exp(-|\tau|/\tau_3)\} (1 - \exp(-|\tau|/\tau_c)) \quad (27)$$

By writing similar expressions for the second and third terms of eq 23, using them in eqs 4-10, and taking the Fourier components (eq 1), the spectral density functions of the anisotropic rotational diffusion of the overall motion with a bistable jump segmental motion are obtained as

$$J_h(\omega) = \frac{1}{2} K_h \Delta \{A_+ f_h(\tau_+) + A_- f_h(\tau_-) + A'_+ f_h(\tau'_+) + A'_- f_h(\tau'_-) + A_{yz} f_h(\tau_1) + A'_{yz} f_h(\tau'_1) + A_{xz} f_h(\tau_2) + A'_{xz} f_h(\tau'_2) + A_{xy} f_h(\tau_3) + A'_{xy} f_h(\tau'_3)\} \quad (28)$$

where $\Delta = \tau_a \tau_b / 2(\tau_a + \tau_b)^2 r_a^3 r_b^3$ and A 's are the amplitudes given by

$$\begin{aligned} A_{\pm} &= 2(\Pi^{ab} \mp \Theta^{ab}) + R_r R_r^{-3} (\Pi^{aa} \mp \Theta^{aa}) + R_r^{-1} R_r^3 (\Pi^{bb} \mp \Theta^{bb}) \\ A'_{\pm} &= -2(\Pi^{ab} \mp \Theta^{ab}) + R_r^{-3} (\Pi^{aa} \mp \Theta^{aa}) + R_r^3 (\Pi^{bb} \mp \Theta^{bb}) \\ A_{ij} &= 2\Gamma_{ij}^{ab} + R_r R_r^{-3} \Gamma_{ij}^{aa} + R_r^{-1} R_r^3 \Gamma_{ij}^{bb} \\ A'_{ij} &= -2\Gamma_{ij}^{ab} + R_r^{-3} \Gamma_{ij}^{aa} + R_r^3 \Gamma_{ij}^{bb} \end{aligned} \quad (29)$$

with $i \neq j = x, y, z$.

$$\begin{aligned} R_r &= \tau_a / \tau_b; \quad R_r = r_a / r_b \\ 1/\tau'_+ &= 1/\tau_+ + 1/\tau_c \\ 1/\tau'_- &= 1/\tau_- + 1/\tau_c \\ 1/\tau'_1 &= 1/\tau_1 + 1/\tau_c \end{aligned}$$

$$\begin{aligned} 1/\tau'_2 &= 1/\tau_2 + 1/\tau_c \\ 1/\tau'_3 &= 1/\tau_3 + 1/\tau_c \end{aligned} \quad (30)$$

and

$$f_h(\tau) = 2\tau / (1 + (h\omega\tau)^2) \quad (31)$$

The spectral density functions depend on ten correlation times for the bistable jump. For an n site jump the spectral density functions will be complicated and the number of correlation times governing the motion will be $5n$, with their corresponding geometrical weighting factors. The n site jump model with $n \rightarrow \infty$, with a Gaussian probability distribution, goes over to the continuous diffusion model having a single correlation time for the internal motion.^{9,10} It may be mentioned here that if the internal motion does not modulate the internuclear distance ($r_a = r_b$) the correlation times in eq 30 remain unaltered but the relative weighting factors of the correlation function are changed. For internal motion involving more than two sites, analytical expressions are complex and numerical calculation of spectral density functions may be preferred. Equation 28 contains spectral density functions for anisotropic overall reorientation which reduce under various simplifications, as described below.

(A) Overall Motion of the Axially Symmetric Ellipsoid. Instead of a complete anisotropic rotational diffusion, if an axially symmetric ellipsoid is assumed then two of the diffusion constants are equal ($\mathcal{R}_2 = \mathcal{R}_3$ resulting in $\tau_2 = \tau_3$ and $\tau'_2 = \tau'_3$). The definitions in eqs 5-10 become

$$\begin{aligned} 1/\tau_1 &= 4\mathcal{R}_1 + 2\mathcal{R}_2, \quad 1/\tau_2 = 1/\tau_3 = \mathcal{R}_1 + 5\mathcal{R}_2 \\ 1/\tau_{\pm} &= 6[\mathcal{R} \pm (\mathcal{R}^2 - \mathcal{L}^2)^{1/2}] \\ \mathcal{L}^2 &= (2\mathcal{R}_1 \mathcal{R}_2 + \mathcal{R}_2^2) / 3 \end{aligned} \quad (32)$$

and eq 28 reduces to the form

$$J_h(\omega) = \frac{1}{2} K_h \Delta \{A_+ f_h(\tau_+) + A_- f_h(\tau_-) + A'_+ f_h(\tau'_+) + A'_- f_h(\tau'_-) + A_{yz} f_h(\tau_1) + A'_{yz} f_h(\tau'_1) + (A'_{xy} + A'_{xz}) f_h(\tau'_2)\} \quad (33)$$

The number of correlation times in this case reduces to eight. Axially symmetric rotational diffusion is an important process of relaxation in long-chain molecules such as α -helix or polymer chain in solution. In such a situation the major axis of the axially symmetric ellipsoid may be assigned to the axis of the helix or the long axis of the polymer chain and Π, Θ , and Γ are obtained by using the Euler angle transformation given in eq 15.

(B) Isotropic Rotational Diffusion. Under the assumption of isotropic random reorientation of the overall molecule, the diffusion constants along the three axes are equal ($\mathcal{R}_1 = \mathcal{R}_2 = \mathcal{R}_3$, resulting in $\tau_1 = \tau_2 = \tau_3 = \tau_+ = \tau_- = \tau_g$ and $\tau'_1 = \tau'_2 = \tau'_3 = \tau'_+ = \tau'_- = \tau'_g$). The global motion can be represented by a single correlation time τ_g given by $1/6\mathcal{R}_1$ and the internal motion by an effective correlation time τ_c . Moreover, for an isotropic rotational diffusion, the various direction cosines calculated in the S_C frame are equal to the direction cosines in the ellipsoidal frame (Euler transformation matrix in eq 15 in a unit matrix). This approximation reduces eq 33 to

$$J_h(\omega) = K_h \Delta [A f_h(\tau_g) + A' f_h(\tau_c)] \quad (34)$$

where

$$\begin{aligned} A &= A_+ + A_- + A_{xy} + A_{xz} + A_{yz} \\ &= ([2\Pi^{ab} + \Gamma_{yz}^{ab} + \Gamma_{xz}^{ab} + \Gamma_{xy}^{ab}] + R_r R_r^{-3} [2\Pi^{aa} + \Gamma_{yz}^{aa} + \Gamma_{xz}^{aa} + \Gamma_{xy}^{aa}] + R_r^3 R_r^{-1} [2\Pi^{bb} + \Gamma_{yz}^{bb} + \Gamma_{xz}^{bb} + \Gamma_{xy}^{bb}]) \end{aligned}$$

and

$$\begin{aligned} A' &= A'_+ + A'_- + A'_{xy} + A'_{xz} + A'_{yz} \\ &= (-[2\Pi^{ab} + \Gamma_{yz}^{ab} + \Gamma_{xz}^{ab} + \Gamma_{xy}^{ab}] + R_r^{-3} [2\Pi^{aa} + \Gamma_{yz}^{aa} + \Gamma_{xz}^{aa} + \Gamma_{xy}^{aa}] + R_r^3 [2\Pi^{bb} + \Gamma_{yz}^{bb} + \Gamma_{xz}^{bb} + \Gamma_{xy}^{bb}]) \end{aligned} \quad (35)$$

with $\tau_c^{-1} = \tau_g^{-1} + \tau_c^{-1}$.

With use of the definitions of Π^{ab} and Γ^{ab} from eq 26 the above equation can be rewritten as

$$J_h(\omega) = \frac{K_h \tau_a \tau_b}{(\tau_a + \tau_b)^2 r_a^3 r_b^3} \left\{ \left[\frac{\tau_a^2 r_b^6 + \tau_b^2 r_a^6}{\tau_a \tau_b r_a^3 r_b^3} + \Omega \right] f_h(\tau_g) + \left[\frac{r_b^6 + r_a^6}{r_a^3 r_b^3} - \Omega \right] f_h(\tau_e) \right\} \quad (36)$$

where

$$\Omega = [3(x_a x_b + y_a y_b + z_a z_b)^2 / r_a^2 r_b^2] - 1 \quad (37)$$

Equation 36 gives the spectral density functions for a bistable jump segmental motion with an overall isotropic motion. The spectral density function in eq 36 can thus be considered as having a contribution from two processes: one describing the overall reorientation of the molecule given by the first term and having a correlation time τ_g and the other given by the second term describing the segmental motion through an effective correlation time, τ_e . For $\beta = 0^\circ$ and 180° , the spin D is collinear with the vector BC about which the internal motion is assumed to take place. In such a circumstance there is no internal motion and the spectral density functions in eq 36 reduce, for $\tau_a = \tau_b$, to

$$J_h(\omega) = K_h f_h(\tau_g) / r_0^6 \quad (38)$$

where r_0 is obtained by using eqs 12–14 as

$$r_0^2 = r_{AB}^2 + (r_{BC} \pm r_1)^2 - 2r_{AB}(r_{BC} \pm r_1) \cos(\angle ABC) \quad (39)$$

with $(r_{BC} + r_1)$ and $(r_{BC} - r_1)$ corresponding to $\beta = 0^\circ$ and 180° , respectively.

For all other values of β , there is internal motion accompanied by a modulation of the internuclear distance in the present model. In order to compare the results of this model to earlier models in which internal motion without modulation of the internuclear distance was assumed, substituting an effective $r_{ab} = r_a = r_b$, eq 36 reduces to the earlier known result^{32,33} as

$$J_h(\omega) = \frac{K_h}{(\tau_a + \tau_b)^2 r_{ab}^6} \{ [\tau_a^2 + \tau_b^2 + \tau_a \tau_b \Omega] f_h(\tau_g) + [\tau_a \tau_b (2 - \Omega)] f_h(\tau_e) \} \quad (40)$$

When the internal motion is fast compared to the overall motion ($\tau_e \ll \tau_g$) and eq 36 is modified with $\tau_e = \tau_c$, both motions contribute to the spectral density functions. However, when the overall motion is fast compared to the internal motion ($\tau_g \ll \tau_e$), $\tau_e = \tau_g$, in other words the spectral density components due to the effective and the overall motion are of the same order [$f_h(\tau_e) \approx f_h(\tau_g)$], eq 36 gives

$$J_h(\omega) = \frac{K_h}{(\tau_a + \tau_b)^2 r_a^6 r_b^6} [\tau_a^2 r_b^6 + \tau_b^2 r_a^6 + \tau_a \tau_b (r_a^6 + r_b^6)] f_h(\tau_g) \quad (41)$$

and the global motion dominates the spectral density function. Further assuming that τ_a and τ_b are equal, eq 41 becomes

$$J_h(\omega) = K_h f_h(\tau_g) \frac{1}{2} \left[\frac{1}{r_a^6} + \frac{1}{r_b^6} \right] \quad (42)$$

Equation 41 shows that the effective spectral density function is proportional to the weighted average of the inverse sixth power of the distances of the two sites, *only when the global and the effective motion are of the same order or equivalently when the overall motion is much faster than the internal motion*. Equation 42 shows that it is a direct average when the two sites are equally populated.

It may be mentioned that for anisotropic reorientation with the assumption that the overall motion is fast compared to internal motion, all the primed correlation times become equal to the corresponding unprimed correlation times ($\tau'_\pm = \tau_\pm$; $\tau'_1 = \tau_1$; $\tau'_2 = \tau_2$; $\tau'_3 = \tau_3$). Under this condition the total spectral density functions (eq 28) reduce to the weighted average of the spectral

density functions for each site undergoing anisotropic reorientation rather than those corresponding to a weighted average of the inverse sixth power of the internuclear distances.⁴⁰

When both relaxing spins are on the side chain undergoing internal motion, the internuclear distance is not modulated but the segmental motion affects relaxation. The spectral density functions corresponding to such a situation are obtained by substitution of $r_{AB} = r_{BC} = 0$ in eq 14 and assuming $\tau_a = \tau_b$, as

$$J_h(\omega) = \frac{K_h}{4r^6} \{ [2 + \Omega'] f_h(\tau_g) + [2 - \Omega'] f_h(\tau_e) \} \quad (43)$$

with

$$\Omega' = 3[\cos^2 \beta + \sin^2 \beta \cos(\alpha_a - \alpha_b)]^2 - 1$$

where r is the internuclear distance and α_a and α_b are the azimuthal angles of the two sites. In this situation, β , the semiangle of the cone of internal rotation, becomes also the angle between the internuclear vector and the axis of internal rotation. When there is no internal motion ($\alpha_a = \alpha_b$ yielding $\Omega' = 2$) or when the overall isotropic motion is fast compared to the internal motion ($f_h(\tau_g) = f_h(\tau_e)$), the spectral density functions reduce to

$$J_h(\omega) = K_h f_h(\tau_g) / r^6 \quad (44)$$

In general, the two-site jump model discussed above can be extended to three-or-more-site jumps, but such a situation is not always reduced to an analytical form and the total number of correlation times involved will also be large. More work is needed to include the multisite jump models and stochastic diffusion of the internal motion.

IV. Results

Steady-state and transient NOE's for two mutually relaxing spins undergoing overall isotropic rotational reorientation and a bistable segmental motion modulating the internuclear distance are calculated in this section. The NOE is calculated for all motional regimes for the global motion and short correlation limit for segmental motion. The NOE is calculated between the spins A and D (Figure 1) with A–B and B–C bond lengths as standard H^β – C^β and C^β – C^γ bond lengths, respectively, and the CD distance (vector r_1) is calculated as 1.367 Å from the standard tryptophan geometry.⁴¹

(A) **Steady-State NOE Experiments.** The two-spin steady-state NOE (η_{ss}) on complete saturation of either one of the spins (A or D, Figure 1) is given by⁴²

$$\eta_{ss} = (W_2 - W_0) / (W_0 + 2W_1 + W_2) \quad (45)$$

where the transition probabilities of dipole–dipole relaxation (W 's) are given by⁴²

$$W_0 = \frac{9}{16} \gamma^4 \hbar^2 J_0(\omega) \quad W_1 = \frac{9}{16} \gamma^4 \hbar^2 J_1(\omega) \\ W_2 = \frac{9}{4} \gamma^4 \hbar^2 J_2(\omega) \quad (46)$$

By substituting for spectral densities from eq 36 along with the equal population of the bistable jump ($\tau_a = \tau_b$), eq 45 becomes

$$\eta_{ss} = \frac{(6W_{2g} - W_{0g}) + (6W_{2e} - W_{0e})}{(6W_{2g} + 3W_{1g} + W_{0g}) + (6W_{1e} + 3W_{1e} + W_{0e})} \quad (47)$$

where $W_{hg} = U_+ f_h(\tau_g)$, $W_{he} = U_- f_h(\tau_e)$, $h = 0, 1$, and 2 and

$$U_\pm = [(r_a^6 + r_b^6) / (r_a^3 r_b^3) \pm \Omega] \quad (48)$$

The steady-state NOE is dependent on both global and effective motions. The NOE is also sensitive to the molecular geometry through the constants U_\pm . Figure 2 shows the steady-state NOE as a function of the semiangle of the cone of internal motion β , for various values of the azimuthal angle α . The calculated NOE for $\omega\tau_g$ equal to 0.1, 1.118, and 10 is shown respectively in Figure 2, a, b, and c. The bistable jump in these calculations is taken

(40) Krishnan, V. V. Ph.D. Thesis, Indian Institute of Science, Bangalore, 1991.

(41) Momany, F. A.; McGuire, R. F.; Burgess, A. W.; Scheraga, H. A. *J. Phys. Chem.* **1975**, *79*, 2361–2381.

(42) Solomon, I. *Phys. Rev.* **1955**, *99*, 559–565.

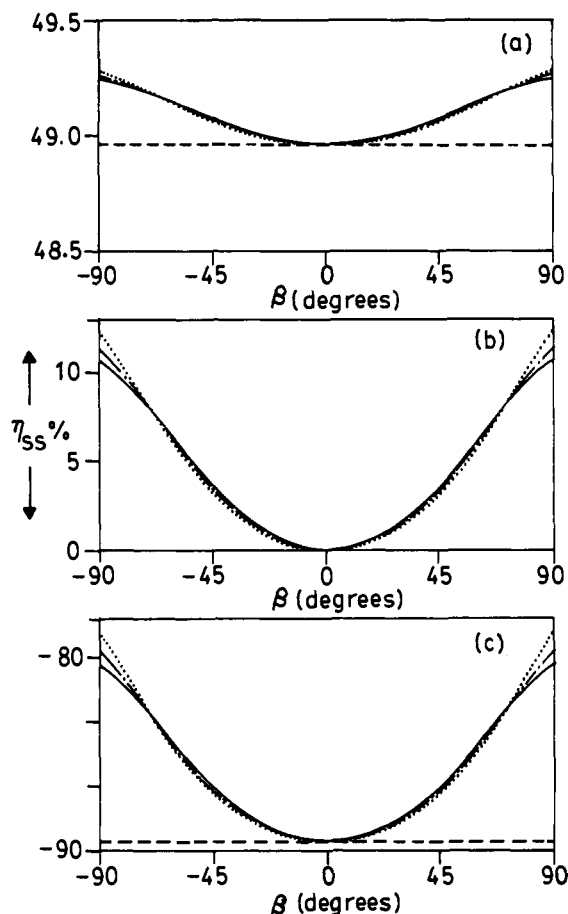


Figure 2. Two-spin steady-state NOE (η_{SS}) defined in eq 47 plotted as a function of β , for different values of $\omega\tau_B$: (a) $\omega\tau_B = 0.1$, (b) $\omega\tau_B = 1.118$, and (c) $\omega\tau_B = 10$, $\omega = 270$ MHz, and for three different values of α , viz. $\alpha = 30^\circ$ (continuous curve), $\alpha = 60^\circ$ (dashed-dotted curve) and $\alpha = 90^\circ$ (dotted curve). The segmental motion is assumed to be in the short correlation limit ($\omega\tau_c = 0.1$) for all the curves and the bistable jump is through 180° . The η_{SS} obtained when an isotropic overall motion without any internal motion is assumed is shown by dashed lines. The dashed line in (b) corresponds to null NOE. These plots are obtained by using the molecular model shown in Figure 1, with $r_{AB} = 1.07$ Å (C-H bond distance), $r_{BC} = 1.54$ Å (C-C bond distance), $r_1 = 1.367$ Å (distance between the C γ carbon to the C7 proton from the standard tryptophan geometry⁴¹), and Δ is assumed to be 30° . For these values the internuclear distance is modulated between the two values 3.268 and 3.635 Å, 2.77 and 3.473 Å and 2.121 and 3.093 Å for $\beta = 30^\circ$, 60° , and 90° , respectively.

as 180° . The two-spin steady-state NOE for isotropic reorientation without internal motion and in the absence of any other relaxation pathway is independent of the internuclear distance and is shown as dashed lines. For $\beta = 0^\circ$ there is no internal motion and, the dashed and full curves coincide. It is noted that the additional segmental motion reduces the effective correlation time in each case, with the exact contribution being geometry (β and α) dependent. The critical correlation regime ($\omega\tau_B = 1.118$) shows most dramatic results by giving 10–12% positive NOE instead of null. From Figure 2, it is also seen that the effect of α , which defines the plane of the bistable jump, is significant only for large values of β , since for small values of β the modulation of the internuclear vector is small for all values of α .

It is evident from the above discussions and Figure 2 that the effect of segmental motion is not negligible in the steady-state NOE experiments. These steady-state NOE results have, however, been obtained strictly for a two-spin system and may not be directly usable in realistic experimental situations without building in additional relaxation pathways or leakage mechanisms. For example, without the leakage mechanism the two-spin steady-state NOE, without internal motion becomes independent of the internuclear distance. In real situations one has often to build in

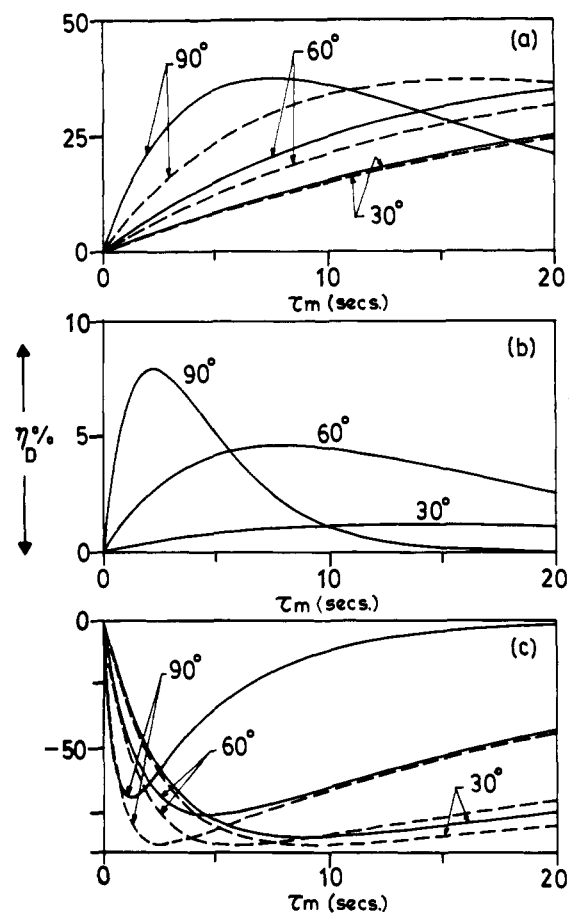


Figure 3. Transient NOE on spin D as a function of the mixing time, when spin A is inverted, for different values of $\omega\tau_B$, (a) 0.1, (b) 1.118, and (c) 10, with $\omega = 270$ MHz and the correlation factor of internal motion being at $\omega\tau_c = 0.1$. The continuous curves show the NOE for three values of β (30° , 60° , and 90°) with modulation of internuclear distances, and the dashed curves correspond to the NOE when the distance between the two bistable sites is assumed to be the average of the distances of the two bistable sites as $r_{av}^{-6} = (r_a^{-6} + r_b^{-6})/2$ and relaxing with a single correlation time (τ_B) without internal motion. The dashed line in (b) corresponds to null NOE. α is zero for all curves. The remaining parameters are the same as in Figure 2.

leakage terms⁴³ or extend the calculation to multispins.

(B) Transient NOE Experiments. In transient NOE experiments, the magnetization of one of the spins is inverted and that of the other is observed as a function of the mixing time (τ_m). When the magnetization of spin A is inverted by a selective pulse at $t = 0$, the deviation of populations from equilibrium ($\chi_i = P_i - P_i^0$) for both spins can be written with use of Solomon's equation as⁴²

$$\begin{aligned} \chi_D(t) &= P_D^0(e^{-(\rho-\sigma)t} - e^{-(\rho+\sigma)t}) \\ \chi_A(t) &= -P_A^0(e^{-(\rho-\sigma)t} + e^{-(\rho+\sigma)t}) \end{aligned} \quad (49)$$

where ρ and σ are the self- and cross-relaxation rates, defined as

$$\rho = W_0 + 2W_1 + W_2 \quad \sigma = W_2 - W_0 \quad (50)$$

The continuous curves in Figure 3 show the NOE on the spin D as a function of the mixing time (τ_m) for three different values of β and for three values of $\omega\tau_B$. The α in all these curves are assumed to be zero and the bistable jump is by 180° . The dashed curve in each case shows the corresponding NOE when the relaxation process is assumed to be governed by an overall correlation time (τ_B) without internal motion, and the distance between the spins is assumed to be $r_{av}^{-6} = (r_a^{-6} + r_b^{-6})/2$. For $\omega\tau_B = 1.118$, the dashed curve is zero for all values of β and τ_m . These results

(43) (a) Duben, A. J.; Hutton, W. C. *J. Magn. Reson.* **1990**, *88*, 60–71.
(b) Duben, A. J.; Hutton, W. C. *J. Am. Chem. Soc.* **1990**, *112*, 5917–5924.

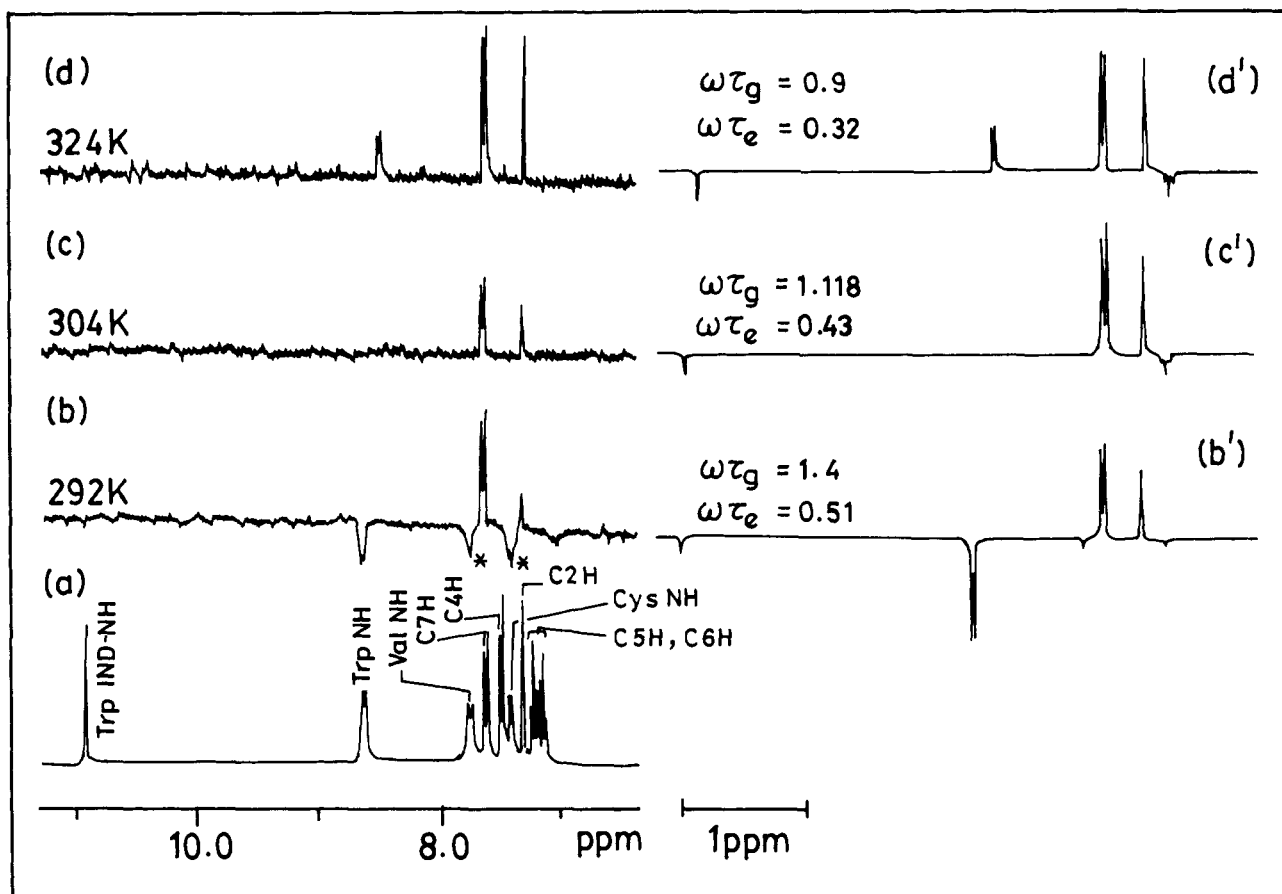


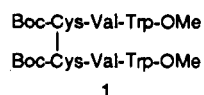
Figure 4. Trace (a) shows the low-field experimental one-dimensional spectrum of **1** at 270 MHz, at 292 K, in dimethyl sulfoxide- d_6 solution. Traces (b), (c), and (d) are the experimental steady-state NOE difference spectra obtained at 292, 304, and 324 K, respectively, when the $C^\beta H$ and $C^\alpha H$ of tryptophan at 3.20 ppm are saturated, and the traces (b'), (c'), and (d') are the corresponding calculated spectra with $\{\omega\tau_g, \omega\tau_e\}$ values as $\{1.4, 0.51\}$, $\{1.118, 0.43\}$, and $\{0.9, 0.32\}$, respectively. The calculated NOE's were obtained by assuming that the overall motion is an isotropic rotational reorientation and the segmental motion a bistable jump by 180° . Negative NOE observed on ValNH (*) and CysNH (*) in trace (b) are due to partial saturation of the corresponding β protons, which resonate near the β protons of tryptophan. All the experimental difference NOE spectra are scaled by 32 with respect to the one-dimensional spectrum (a), and the number of transients accumulated is 128, except in trace (b) where the number is 256 with a relaxation delay of 3 s. All the calculated spectra are plotted in the same arbitrary scale. While in the experimental spectra the NH resonances are broader than the ring proton resonances, in the calculated spectra an equal line width of 2 Hz was used for all the lines.

show that the internal motion has a significant effect on the transient NOE as well as on the recovery of the inverted spin (curves not shown). The segmental motion is to reduce the effective correlation time in each case.

These results suggest that the observed NOE on a spin without considering the details of the internal motion along with the relaxation process may lead to significantly different results. The differences introduced in the NOE buildup curves are large even for small mixing times and increase with β .

V. Experimental Results

Figure 4 shows the steady-state NOE spectra of the tryptophan containing polypeptide



Trace a of Figure 4 shows the low-field region of the one-dimensional spectrum recorded on a Bruker 270-MHz FT NMR spectrometer equipped with a Aspect-2000 computer. Traces b-d correspond to the temperature dependence of the steady-state NOE when the C^β protons of tryptophan are saturated. At room temperature (Figure 4b) negative NOE on the backbone proton of Trp NH and positive NOE on the ring protons (Trp C7H and Trp C2H) is observed. On increasing the temperature to 304 K (Figure 4c) the backbone proton shows null NOE while the ring protons continue to show positive NOE. On further increase of temperature to 324 K (Figure 4d), both the backbone and the

ring protons show positive NOE. These observations indicate that at 304 K the overall reorientation of the peptide is near the null region such that $\omega\tau_g \approx 1.118$ while the segmental motion is such that $\omega\tau_e < 1.118$. At lower temperatures $\omega\tau_g > 1.118$ and at higher temperatures $\omega\tau_g < 1.118$, with $\omega\tau_e$ remaining less than 1.118 for all three temperatures. The room temperature steady-state NOE spectrum (Figure 4b) of this molecule was also reported earlier, where it was correctly suggested that the simultaneous observation of positive and negative NOE was due to the presence of segmental motion.⁸ In ref 8, no detailed calculation of the NOE intensities was performed, which is done in this work on the basis of the model proposed here. The details of the conformation and the calculation are as follows.

The NMR studies of this molecule suggested an antiparallel β -sheet conformation in the liquid state.⁴⁴ Figure 5 shows a portion of the molecule in which the backbone is in an antiparallel β -sheet conformation. The coordinates of the molecule are generated from the standard ψ and ϕ values of an *ideal* antiparallel β -sheet. The axis of overall orientation is assumed to be along the Val- C^α and Trp- C^α carbons of the backbone, while the segmental motion is about the C^β - C^γ bond axis of the tryptophan (Figure 5). The angle Δ is the angle between these two axes. The semiangle of the cone of internal rotation (β) for tryptophan and the various internuclear vectors in two states differing by 180° calculated from the geometry are listed in Table 1.

(44) Balam, H.; Uma, K.; Balam, P. *Int. J. Protein Peptide Res.* **1990**, *35*, 495-500.

Table I. Geometrical Parameters from Figure 5

For the Internuclear Vectors between Backbone and Side Chain				
internuclear vector		β , deg	$r_{\text{site I}}$, Å	$r_{\text{site II}}$, Å
from	to			
Trp NH	C2H	75.75	4.98	5.01
	Ind NH	21.76	6.85	6.86
	C4H	15.89	7.99	8.00
	C5H	41.99	8.23	8.26
	C6H	69.02	6.86	6.90
	C7H	85.93	5.05	5.09
	Trp C α H	C2H	75.75	4.35
Ind NH		21.76	6.17	6.18
C4H		15.89	7.31	7.32
C5H		41.99	7.60	7.62
C6H		69.02	6.30	6.34
C7H		85.93	4.47	4.50
Trp C β H		C2H	75.75	3.34
	Ind NH	21.76	5.04	5.05
	C4H	15.89	6.18	6.19
	C5H	41.99	6.57	6.58
	C6H	69.02	5.44	5.46
	C7H	85.93	3.58	3.60
	Trp C γ H	C2H	75.75	3.32
Ind NH		21.76	5.03	5.04
C4H		15.89	6.16	6.17
C5H		41.99	6.55	6.57
C6H		69.02	5.43	5.45
C7H		85.93	3.57	3.59

For the Internuclear Vectors among the Side Chain			
internuclear vector		β , deg	r_{ab} , Å
from	to		
C2H	Ind NH	26.53	2.71
	C4H	40.87	4.85
	C5H	58.72	6.36
	C6H	79.72	6.43
	C7H	81.69	4.95
	Ind NH	62.02	2.64
	C5H	78.98	4.57
C4H	C6H	76.52	5.5
	C7H	51.22	5.02
	C5H	80.91	2.3
	C6H	57.55	4.05
C5H	C7H	22.08	4.73
	C6H	22.71	2.33
C6H	C7H	8.49	4.06
	C7H	37.62	2.35

Multispin NOE calculations were performed by including all the protons of the Cys-Val-Trp backbone and side chains utilizing the generalized Solomon's equations. In these calculations, it is assumed that the overall motion is an isotropic reorientation and the segmental motion is a bistable jump by 180° with $\alpha = 0$ and $\tau_a = \tau_b$. The spectral density functions for the protons within the ring of the tryptophan that undergo a bistable jump are obtained from eq 43, and the relaxation of the dipolar vectors between the backbone and the side chain is governed by the spectral density functions given in eq 36. The results of the calculations are shown in Figure 4 (b', c', and d') with the parameters given in the caption. The calculated spectra show good correspondence with the experimental spectra.

These results show that the segmental motion affects the steady-state NOE. The calculated spectra confirm the validity of the proposed model for the segmental motion in aromatic side chains. This type of model-based calculation can also be performed for transient and two-dimensional NOE experiments where it can be utilized for back calculations of the structure from the observed NOE.

It may be mentioned that while the proposed model satisfactorily explains the observed experimental NOEs and their time dependences, it may be possible to obtain reasonable fits to the experimental data by other approaches, such as a phenomenological two-correlation time model or other model-free approaches. However, the advantage of a detailed model-based calculation is

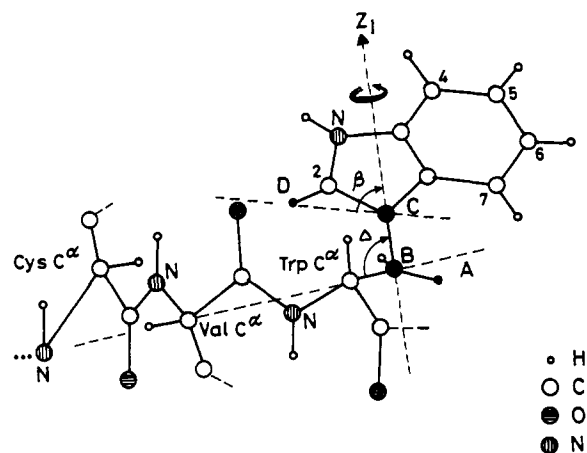


Figure 5. Portion of molecule 1 in the antiparallel β -sheet conformation. The proton coordinates of the molecule are generated by assuming the standard ϕ and ψ values corresponding to an ideal antiparallel β -sheet conformation ($\phi = -139^\circ$ and $\psi = 135^\circ$). The axis of the overall motion is assumed to be along the line joining the ValC α to TrpC α carbons and the axis of internal motion is along the C β -C γ bond axis (BC) of the tryptophan. The angle between these two axes (Δ) is calculated as 88° and according to the present model; it is the same for the dipolar vectors between the backbone and the ring protons. Any two protons in the molecule can be fit into the model discussed in Figure 1, and one such fragment, A(Trp C β H), B(Trp C β H), C(Trp C γ H), and D(Trp C β H), is also shown. In this calculation it is assumed that the segmental motion takes place only around the C β -C γ axis of tryptophan, while the rest of the molecule is rigid. The various internuclear distances and the semiangles of the cone of internal motion (β) calculated from the geometry are listed in Table I.

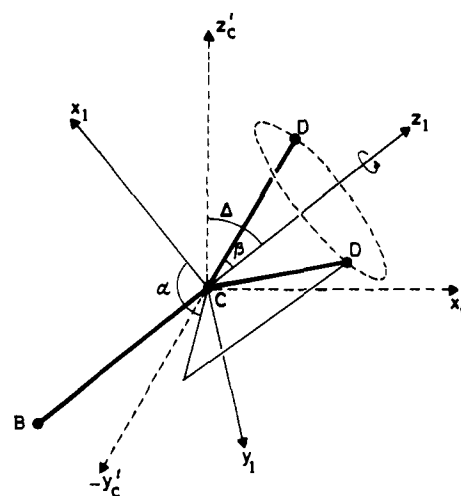


Figure 6. Part of the molecular fragment containing the atoms B, C, and D only. The atom D undergoes a bistable jump internal motion about Z_1 through an angle β , polar angle of r_1 in S_1 , and an azimuthal angle α (α_a and α_b corresponds to the two sites of the bistable jump motion). The frame $S'_C(X'_C, Y'_C, Z'_C)$ is the same as frame $S_C(X_C, Y_C, Z_C)$, except the origin shifted from atom A to C. X and Z axes of the frames S_1 and S'_C are on the same plane while the Y axes are out of phase by 180° .

that (i) it is possible to get more accurate fit to more complex relaxation or NOE data and (ii) it provides a detailed physical picture of the internal motions.

VI. Conclusions

A model for segmental motion superimposed on an overall anisotropic reorientation has been developed, with the segmental motion being a bistable jump modulating the internuclear distances. This model has been utilized for explaining the simultaneous observation of positive and negative NOE and its temperature dependence in a peptide. The calculated spectra yield satisfactory correspondence with the observed experimental spectra and confirm the basic features of the model. While this paper

assumes only a bistable jump by 180°, other internal motions such as rotations by other angles, free rotations, vibrations, and distortions can also occur in a molecule. These need detailed calculations using numerical methods like molecular mechanics and Monte Carlo simulation.

In NOE calculations involving more than two spins, the cross-correlation between the different dipolar vectors often plays a significant role.⁴⁵ When an internal motion is also present apart from the overall motion, the cross-correlation spectral density functions have additional information about the correlation between the two motions. The present model assumes that the global and segmental motions are independent of each other, hence multispin NOE have been calculated in this paper by neglecting the cross-correlation effects.

Acknowledgment. Discussions with Prof. B. D. Nageswara Rao and Prof. P. Balaram, who also provided the peptide sample, are gratefully acknowledged. We thank Profs. C. L. Khetrpal and J. Tropp for perusal of the manuscript. A.K. acknowledges the Department of Science and Technology, India, for a research grant and V.V.K. acknowledges CSIR for a senior research fellowship.

Appendix: Direction Cosines of the Dipolar Vector in the Internal Frame

The coordinates of the nucleus D (tip of the vector \vec{r}_1) at any time t in the $S_1(X_1, Y_1, Z_1)$ are

(45) (a) Krishnan, V. V.; Anil Kumar J. *Magn. Reson.* 1991, 92, 293-311.
(b) Dalvit, C.; Bodenhausen, G. *Adv. Magn. Reson.* 1990, 14, 1-33.

$$\begin{aligned} x_1(t) &= r_1 \sin \beta \cos \alpha(t) & y_1(t) &= r_1 \sin \beta \sin \alpha(t) \\ z_1(t) &= r_1 \cos \beta \end{aligned} \quad (A1)$$

where α is the azimuthal of the \vec{r}_1 vector as shown in Figure 6. Consider a frame of reference $S'_C(X'_C, Y'_C, Z'_C)$, the same as the reference frame of convenience $S_C(X_C, Y_C, Z_C)$ except the origin is shifted from atom A to C where S_C is the frame of convenience with the origin at atom A as defined in Figure 1. The frame of convenience is taken such that the X_1 and Z_1 axes are in the same plane as the X'_C and Z'_C axes and the two Y axes are 180° out of phase (Figure 6). The transformation from S'_C to S_1 is given by

$$\begin{bmatrix} x'_C(t) \\ y'_C(t) \\ z'_C(t) \end{bmatrix} = \begin{bmatrix} -\cos \Delta & 0 & \sin \Delta \\ 0 & -1 & 0 \\ \sin \Delta & 0 & \cos \Delta \end{bmatrix} \begin{bmatrix} x_1(t) \\ y_1(t) \\ z_1(t) \end{bmatrix} \quad (A2)$$

where Δ is the angle between the Z_1 and the Z'_C or equivalently in terms of the geometry of the molecular fragment, given by $(\angle ABC) - \pi/2$. On translating the origin from atom C to A the coordinates of nucleus D in the frame S_C are

$$\begin{aligned} x_C(t) &= r_{AB} + r_{BC} \sin \Delta + x'_C(t) & y_C(t) &= y'_C(t) \\ z_C(t) &= r_{BC} \cos \Delta + z'_C(t) \end{aligned} \quad (A3)$$

eqs 12-15 in the text are obtained by substituting eqs A1 and A2 in eq A3.

Solution Structure of a Synthetic N-Glycosylated Cyclic Hexapeptide Determined by NMR Spectroscopy and MD Calculations[†]

H. Kessler,* H. Matter, G. Gemmecker, A. Kling, and M. Kottenhahn

Contribution from the Organisch-Chemisches Institut, Technische Universität München, Lichtenbergstrasse 4, D-8046 Garching, Germany. Received January 17, 1991

Abstract: The synthesis and conformational analysis by NMR spectroscopy and MD calculations of the N-glycosylated cyclic hexapeptide cyclo(-D-Pro-Phe-Ala-[N-2-acetamido-2-desoxy- β -D-glucopyranosyl])Gln-Phe-Phe- (I) and the cyclic hexapeptide precursor cyclo(-D-Pro-Phe-Ala-Glu(OtBu)-Phe-Phe-) (II) were carried out to study the influence of N-glycosylation on conformation of peptides. For both compounds, all of the distance constraints derived from 2D NOE measurements could not be satisfied by one conformation. Therefore, second conformers interconverting fast compared to the NMR time scale are assumed. The two conformations differ in the β -turn structure between Ala³ and Phe⁶ (β II- or β I-turns, respectively). The β 11'-turn about amino acids D-Pro¹ and Phe² is highly conserved in both MD simulations. The conformations were refined by using restrained MD simulations in vacuo and in water. Additional MD simulations with application of time-dependent distance constraints provide further information about the internal flexibility of I. The conformational equilibrium could be confirmed; several conformational changes were detected evidenced by a large number of torsion angle fluctuations during the time scale of the simulation. Both proposed backbone conformers were significantly populated. The averaging over coupling constants and NOE data reveal the high flexibility of the structure and the good agreement with experimental data for both I and II. The N-glycosylation does not affect the conformation or the overall shape of the peptide backbone or side chains. It has no influence on the hydrogen-binding pattern or on the fast dynamical equilibrium of the molecule.

Introduction

Carbohydrates and glycoproteins are of great importance in biological recognition phenomena.¹ Therefore, the interest in the synthesis and conformations of glycopeptides as partial structures

of glycoproteins has increased considerably.² Many applications for glycopeptides are currently being established, e.g., in the development of selective pharmaceuticals and for the improvement of pharmacokinetic properties.³

Presently, very little is known about the mutual conformational influences between the protein or peptide structures and the

[†] Abbreviations: BOC, *tert*-butoxycarbonyl; COLOC, heteronuclear correlation via long-range couplings; DQF-H,H-COSY, double quantum filtered proton-correlated spectroscopy; E-COSY, exclusive correlated spectroscopy; EDCI, *N*-ethyl-*N'*-(dimethylamino)propylcarbodiimide hydrochloride; HMBC, heteronuclear multiple bond correlation; HMQC, heteronuclear multiple quantum coherence correlation; HOBt, 1-hydroxybenzotriazole; solvent A, *n*-butanol/H₂O/acetic acid (3:1:1); solvent B, chloroform/methanol (9:1); solvent C, chloroform/methanol/acetic acid (95:5:3); NOE, nuclear Overhauser effect; NOESY, nuclear Overhauser and exchange spectroscopy; ROE, rotating frame NOE; ROESY, rotating frame Overhauser and exchange spectroscopy; TOCSY, total correlation spectroscopy; Z, benzyloxy-carbonyl.

(1) (a) Feizi, T. *Nature* 1985, 314, 53-57. (b) Goldstein, E. J. Carbohydrate Protein Interaction. *ACS Symp. Ser.* 1979, No. 88.

(2) (a) Meyer, B. *Top. Curr. Chem.* 1990, 154, 141-208. (b) Paulsen, H. *Angew. Chem.* 1990, 102, 851-67. (c) Schmidt, R. R. *Angew. Chem.* 1986, 25, 213-236. (d) Kunz, H. *Angew. Chem.* 1987, 99, 297-311.

(3) (a) Gabius, H. J. *Angew. Chem.* 1988, 100, 1321-1330. (b) Bundle, D. R. 14th International Carbohydrate Symposium (Stockholm/Sweden) 14.8.-19.8.1988.